

# We are IntechOpen, the world's leading publisher of Open Access books Built by scientists, for scientists

6,900

Open access books available

186,000

International authors and editors

200M

Downloads

Our authors are among the

154

Countries delivered to

TOP 1%

most cited scientists

12.2%

Contributors from top 500 universities



WEB OF SCIENCE™

Selection of our books indexed in the Book Citation Index  
in Web of Science™ Core Collection (BKCI)

Interested in publishing with us?  
Contact [book.department@intechopen.com](mailto:book.department@intechopen.com)

Numbers displayed above are based on latest data collected.  
For more information visit [www.intechopen.com](http://www.intechopen.com)



# Joint Cooperative Shared Relaying and Multipoint Coordination for Network MIMO in 3GPP LTE-Advanced Multihop Cellular Networks

Anthony Lo and Peng Guan  
*Delft University of Technology  
The Netherlands*

## 1. Introduction

LTE-Advanced (Parkvall et al., 2011; 3GPP TR36.814) is the successor of LTE (Long Term Evolution), which is specified by the Third Generation Partnership Project (3GPP). LTE-Advanced can provide downlink and uplink peak rates up to 1 Gb/s and 500 Mb/s, respectively, in 100 MHz of bandwidth. Similar to its predecessor, LTE-Advanced is an Orthogonal Frequency Division Multiplexing (OFDM)-based radio access technology, with conventional OFDM on the downlink and Discrete Fourier Transform Spread OFDM (DFTS-OFDM) in the uplink. In addition, LTE-Advanced includes several new key technological components, namely carrier aggregation, enhanced MIMO (Multiple-Input Multiple Output), Coordinated MultiPoint transmission and reception (CoMP), and relaying. In this chapter, we focus on the CoMP component and the relaying component.

CoMP is a means of coordinating the transmission and reception of data from/to a single mobile terminal using several geographically distributed base stations. Essentially, CoMP eliminates inter-cell interference by effectively having the multiple base stations act as a single transceiver. CoMP is especially effective for improving data rates of cell-edge mobile terminals where performance is degraded due to inter-cell interference since LTE-Advanced uses full-frequency reuse. Relaying is employed as a low-cost solution to enhance cell-coverage and -capacity. With relaying, the mobile terminal communicates with the base station via a relay node that is wirelessly connected to the base station using the same radio resources as for the mobile terminal that is directly connected to the base station. An LTE-Advanced relay node is divided into a transparent type and a non-transparent type. The main difference between the two types is in the amount of functionality and intelligence included in the relay node. A non-transparent relay node has more functionality and intelligence than a transparent one. This means it is also costlier. The simplest and the cheapest transparent relay is known as Amplify and Forward (AF).

The aim of this chapter is to leverage and combine the benefits of CoMP and relaying in order to improve the performance of cell-edge users, which is severely degraded due to inter-cell interference. The joint relaying and CoMP technique can yield performance gains

beyond what can be achieved using either one of the techniques alone. With the joint relaying and CoMP technique, an AF relay node is deployed at the intersection of two or more cells. The relay node amplifies and retransmits the received signals from multiple base stations to multiple mobile terminals in the downlink. In addition to the relayed signals, the mobile terminals also make use of the direct signals from the base stations to attain cooperative diversity. The coordinating base stations and the relay node form a network MIMO system. Our joint relaying and CoMP technique supports multi-user transmissions using precoding at the transmit side to precancel the co-channel interference. In order to evaluate the performance of the joint relaying and CoMP, we derive expressions for its achievable rates and compare them with the rates of CoMP.

## 2. LTE-Advanced multi-hop cellular network

Fig. 1 shows an overview of the network architecture of LTE-Advanced Multi-hop Cellular Networks (MCN), which is a flat all-IP network. The main architectural elements are the Mobility Management Entity and Gateway (MME/GW), the evolved Node B (eNB), the Relay Node (RN) and the User Equipment (UE). The eNB, which is a base station, connects to the MME/GW by the S1 interface through many-to-many relationship. Each eNB also connects to the neighbouring eNBs via the X2 interface, enabling direct communications. The RN is wirelessly connected to the eNB via the Un interface. A mobile terminal, which is the UE, connects to an RN via the Uu interface. In the case of direct communication, the UE connects to the eNB utilizing the same interface, Uu. In a cell, each eNB serves a number of RNs and UEs, which forms a tree structure with the eNB as the parent. The number of relays in a multi-hop chain is  $n - 1$  for  $n$  number of hops. The complexity is related to the number of hops. Thus, 3GPP has limited  $n$  to two hops for LTE-Advanced MCN. In the rest of the chapter, we refer to the connection between an eNB and an RN as Relay Link (RL), the connection between an RN and a UE as Access Link (AL), and the connection between an eNB and a UE as Direct Link (DL).

### 2.1 Types of RNs

In LTE-Advanced MCN (3GPP TR36.814, 2010), depending on the number of protocol layers used to forward user data, an RN can be classified into a transparent type and a non-transparent type. A transparent RN is invisible to the UE. In other words, the RN just expands the cell coverage of the donor eNB. A transparent RN includes Amplify-and-Forward (AF) (Berger et al., 2009), Decode-and-Forward (DF) (Laneman et al., 2004), Compress-and-Forward (CF) (Kramer et al., 2005) and Estimate-and-Forward (EF) (Cover & El Gamal, 1979). AF amplifies before forwarding the received signal to the destination. DF decodes and re-encodes the received signal before it is forwarded. In CF, the RN compresses the source signal and forwards it to the destination without decoding it. An EF relay forwards an estimate of the received signal to the destination. A non-transparent RN appears as a mini-eNB to the UE. The non-transparent RN is also known as self-backhauling RN (Hoymann et al., 2008).

Irrespective of the relay class, an RN can operate in either full-duplex mode or half-duplex mode. A full-duplex RN can transmit and receive simultaneously, while a half-duplex RN alternate between transmitting and receiving states. The RL can operate on an orthogonal frequency band or share the same frequency band with the AL. The former is referred to as

out-band RN while the latter as in-band RN. An in-band RN can have higher spectral efficiency than out-band RNs. However, it suffers from self-interference. Therefore, adequate isolation must be achieved between the transmitting part of one link and the receiving part of the other link. A half-duplex RN always transmits and receives on orthogonal channels typically in the time domain.

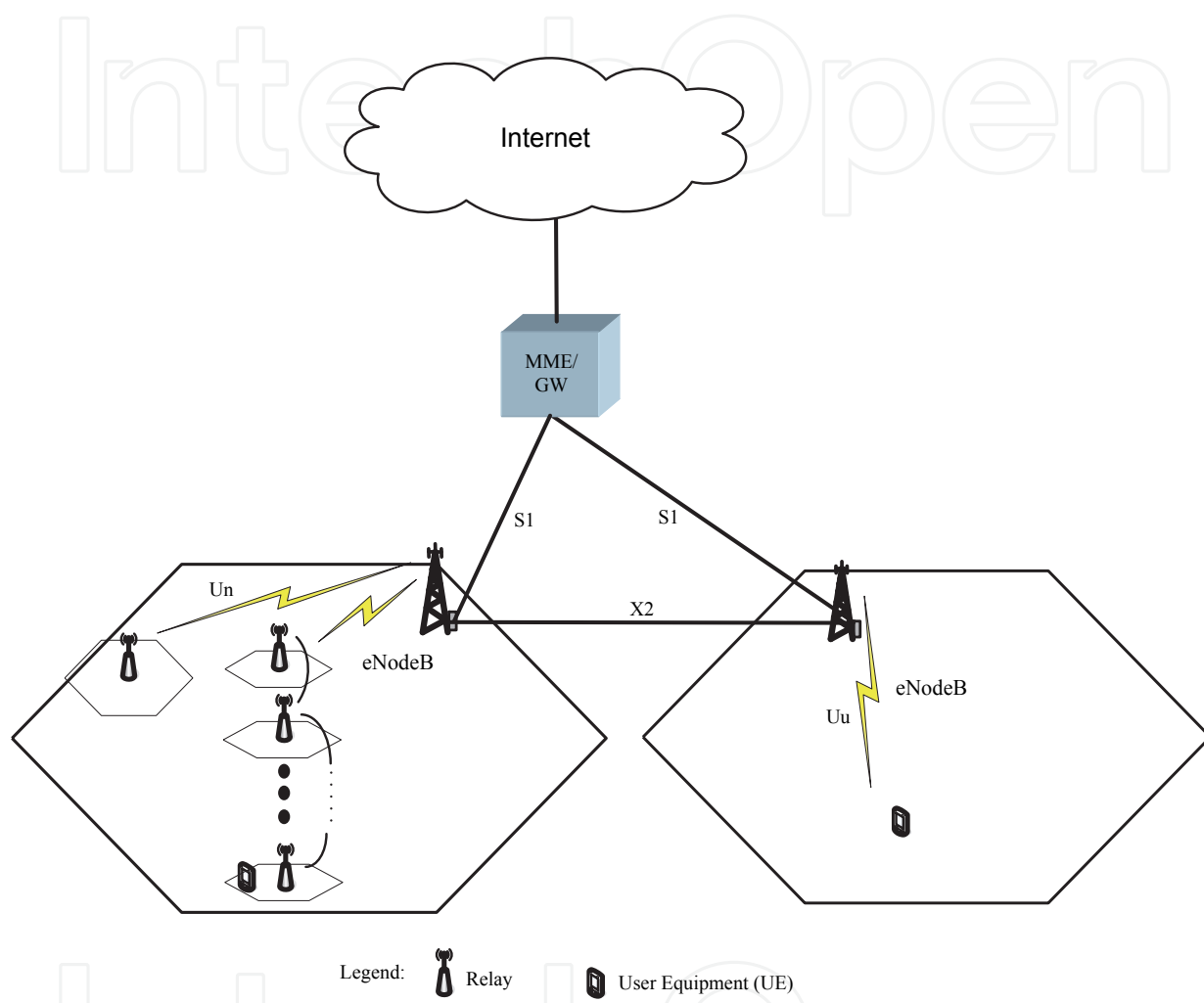


Fig. 1. LTE-Advanced Multi-hop Cellular Architecture

## 2.2 Coordinated Multipoint transmission and reception (CoMP)

LTE-Advanced uses full frequency reuse, which in turn leads to inter-cell interference. CoMP aims at mitigating the inter-cell interference and hence improves spectral efficiency of cell-edge users. Fig. 2 shows the CoMP architecture. The same spectrum resources are used in all cells, leading to interference for UEs at the edge between the cells, where signals from multiple eNBs are received with similar signal power in the downlink. Multiple eNBs can cooperate to mitigate the inter-cell interference. The eNBs are interconnected by the interface X2. Physically, this could be a direct fast fibre link. CoMP can be applied both in the uplink and the downlink. In the downlink, CoMP can be divided into two schemes:

- Joint Processing: user data to be transmitted to a single UE is available at each transmission, i.e., eNB.
- Coordinated scheduling and beamforming: user data is always transmitted from one eNB only, but user scheduling and beamforming decisions are made with coordination among cells.

In the CoMP uplink, multipoint reception implies coordination among multiple, geographically distributed eNBs. Uplink CoMP reception involves joint reception of the transmitted signal at multiple reception points and/or coordinated scheduling decisions among cells to control interference.

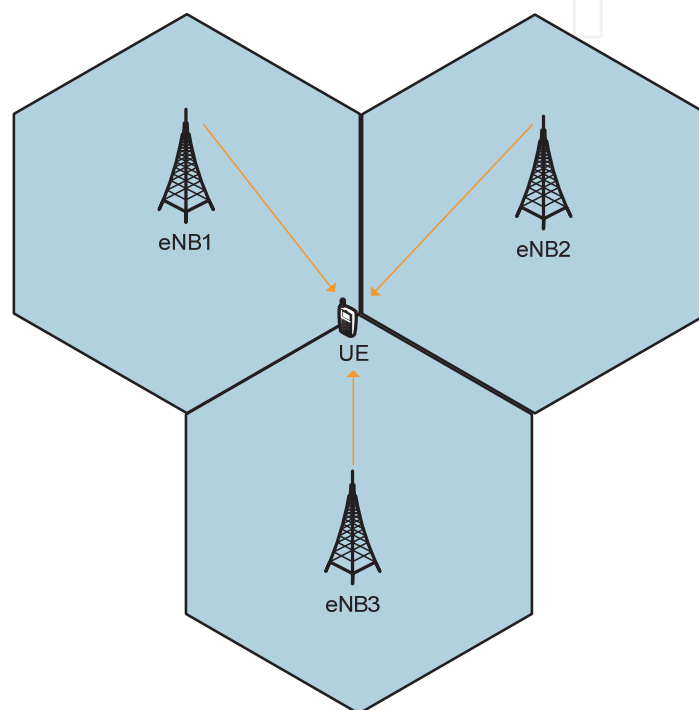


Fig. 2. CoMP Architecture

### 3. Joint cooperative shared relaying and Coordinated Multipoint transmission/reception

In this section, we leverage the benefits of the CoMP and the relaying techniques. The aim of the combined technique is to increase the cell-edge user data rates beyond what can be achieved by using either one of the techniques alone. Unlike users that are close to the eNB, cell-edge users experience lower signal strength because of the distance from the eNB and higher interference levels due to neighbouring eNBs. Furthermore, increasing transmission power does not necessarily lead to higher data rates due to an increase in inter-cell interference level. With the combined technique, an RN is employed to enhance the signal strength and CoMP to mitigate inter-cell interference due to neighbouring eNBs. The combined technique places an RN at the intersection of two or more cells. We propose a full-duplex AF RN for its high spectral efficiency. In the downlink, the RN amplifies and retransmits the received signals from the intersecting eNBs to multiple users. In the uplink,

the RN amplifies and retransmits the received signals from multiple users to all intersecting eNBs. In either uplink or downlink, the destination (namely, UE in the downlink and eNB in the uplink) combines the relayed signal and the direct signals from all the sources (namely, eNB in the downlink and UE in the uplink). The RN and the sources form a network MIMO system. Such an RN is referred to as cooperative relay.

### 3.1 System model

Our system model considers an arbitrary hexagonal cellular network. The eNBs are located in the centre of each cell. The eNBs are grouped into  $L$  clusters. A cluster is composed of a single RN that is shared by  $M$  eNBs and  $K$  UEs. The eNB, the RN and the UE are equipped with one antenna element. In the downlink, each of the  $M$  eNBs transmits data streams of  $K$  UEs at the same time-frequency resources. In the uplink, the  $K$  UEs transmit to the  $M$  eNBs using the same time-frequency resources.

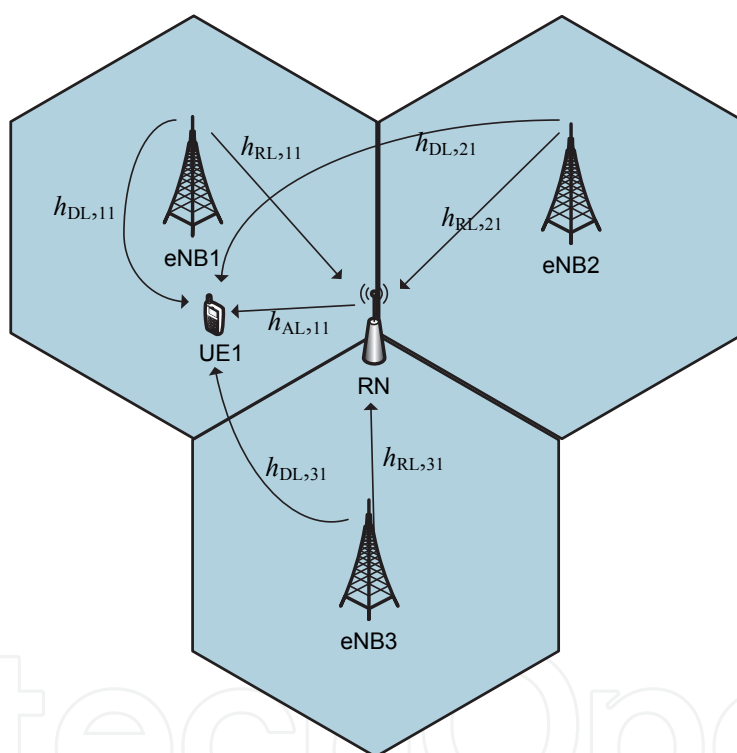


Fig. 3. A System Model for Joint Cooperative Shared Relaying and CoMP

Fig. 3 shows a typical cluster for joint cooperative shared relay and CoMP under the hexagonal cellular model. The relay RN which belongs to the  $l$ th cluster is placed at the corner of three adjacent cells. Thus, for this configuration,  $M = 3$  and  $K = 1$ . In subsections 3.1.1 and 3.1.2, we derive the capacity equations for the downlink and uplink, respectively. The rest of the chapter uses the following notation. Bold uppercase letters  $\mathbf{A}$  denote matrices, bold lowercase letters  $\mathbf{a}$  denote column vectors, and italic lowercase letters  $a$  denote scalars.  $\mathbf{I}$  denotes the identity matrix,  $\mathbf{A}^T$  is the transpose of matrix  $\mathbf{A}$ ,  $\mathbf{A}^*$  is the Hermitian transpose of matrix  $\mathbf{A}$ ,  $\varepsilon$  is expectation operator,  $\min\{x, y\}$  is the minimum of  $x$  and  $y$ ,  $|z|$  is the modulus of complex number  $z$ , and  $\|\mathbf{h}\|$  is the Euclidean norm of vector  $\mathbf{h}$ .

### 3.1.1 Capacity of the joint CoMP and relaying

#### 3.1.1.1 Downlink capacity

The signal received by RN is given by

$$\begin{aligned} y_{RN,l} &= \sum_{m=1}^M h_{RL,ml} x_{eNB,m} + n_{RN,l} \\ &= \mathbf{h}_{RL} \mathbf{x}_{eNB} + n_{RN,l} \end{aligned} \quad (1)$$

where  $\mathbf{h}_{RL} = [h_{RL,1l} \ h_{RL,2l} \ \dots \ h_{RL,ml}]$  is the  $1 \times M$  RL channel vector (where  $h_{RL,ml}$  corresponds to the complex-valued, channel gain between the  $m$ th eNB and the RN, which takes into account path loss),  $\mathbf{x}_{eNB} = [x_{eNB,1} \ x_{eNB,2} \ \dots \ x_{eNB,M}]^T$  is the  $M \times 1$  vector of the transmitted signal ( $x_{eNB,m}$  is the signal transmitted by the  $m$ th eNB), and  $n_{RN,l}$  is the additive white Gaussian noise observed at RN. The power of this noise term is  $\varepsilon\{|n_{RN,l}|^2\} = \sigma_{RN,l}^2$ . The signal received at the  $k$ th UE is a superposition of all the signals transmitted by eNBs and the RN, which is given by

$$\begin{aligned} y_{UE,k} &= \sum_{m=1}^M h_{DL,mk} x_{eNB,m} + h_{AL,ik} g y_{RN,l} + n_{UE,k} \\ &= \sum_{m=1}^M (h_{DL,mk} + g h_{AL,ik} h_{RL,ml}) x_m + (g h_{AL,ik} n_{RN,l} + n_{UE,k}), \quad k = 1, 2, \dots, K \end{aligned} \quad (2)$$

where  $h_{AL,ik}$  corresponds to the complex-valued, channel gain (which includes path loss, shadowing and Rayleigh fading) between the RN and the  $k$ th UE,  $n_{UE,k}$  is the additive white Gaussian noise with power equals to  $\varepsilon\{|n_{UE,k}|^2\} = \sigma_{UE,k}^2$ , and  $g$  is the amplification gain of RN, which is defined as

$$g = \sqrt{\frac{P_{RN,l}}{\sum_{m=1}^M P_{eNB,m} |h_{RL,ml}|^2 + \sigma_{RN}^2}} > 1 \quad (3)$$

$P_{RN,l} = \varepsilon\{|g y_{RN,l}|^2\}$  and  $P_{eNB,m} = \varepsilon\{|x_{eNB,m}|^2\}$  in Equation (3) are the transmit power of the RN and the  $m$ th eNB, respectively. Equation (2) can be expressed as

$$y_{UE,k} = (\mathbf{h}_{DL,k} + g h_{AL,ik} \mathbf{h}_{RL}) \mathbf{x}_{eNB} + \tilde{n} \quad (4)$$

where  $\mathbf{x}_{eNB}$  is similar to the transmitted signal vector of Equation (1),  $\mathbf{h}_{RL}$  is the RL channel vector as in Equation (1),  $\mathbf{h}_{DL,k} = [h_{DL,1k} \ h_{DL,2k} \ \dots \ h_{DL,Mk}]$  is the  $1 \times M$  DL channel vector ( $h_{DL,mk}$  corresponds to the complex-valued, channel gain which includes path loss, shadowing and Rayleigh fading) between the  $m$ th eNB and the  $k$ th UE, and

$\tilde{n} = g h_{AL,ik} n_{RN,l} + n_{UE,k}$  is effective noise term. The power of the effective noise term is  $\varepsilon\{|\tilde{n}|^2\} = |g|^2 |h_{AL,ik}|^2 \sigma_{RN,l}^2 + \sigma_{UE,k}^2$ .

For  $K$  UEs, we can represent the network MIMO channels in the downlink by a system of linear equations as

$$\underbrace{\begin{bmatrix} y_{UE,1} \\ y_{UE,1} \\ \vdots \\ y_{UE,K} \end{bmatrix}}_{\mathbf{y}_{UE}} = \underbrace{\begin{bmatrix} \mathbf{h}_{DL,1} + gh_{AL,11} \mathbf{h}_{RL} \\ \mathbf{h}_{DL,2} + gh_{AL,12} \mathbf{h}_{RL} \\ \vdots \\ \mathbf{h}_{DL,K} + gh_{AL,1K} \mathbf{h}_{RL} \end{bmatrix}}_{\mathbf{H}} \underbrace{\begin{bmatrix} x_{eNB,1} \\ x_{eNB,2} \\ \vdots \\ x_{eNB,K} \end{bmatrix}}_{\mathbf{x}_{eNB}} + \underbrace{\begin{bmatrix} gh_{AL,11} n_{RN,1} + n_{UE,1} \\ gh_{AL,12} n_{RN,1} + n_{UE,2} \\ \vdots \\ gh_{AL,1K} n_{RN,1} + n_{UE,K} \end{bmatrix}}_{\mathbf{n}} \quad (5)$$

For multiuser transmission and reception, the transmitted signal vector  $\mathbf{x}_{eNB}$  in Equation (5) is generated by a weighted linear combination of data symbols contained in a  $K \times 1$  vector  $\mathbf{d} = [d_1 \ d_2 \ \dots \ d_K]^T$ , where  $d_k$  is the specific data symbol intended for the  $k$ th UE. Thus, the  $k$ th UE receives its own symbols as well as the other users' symbols. If the channel state information is perfectly known by each eNB then the zero-forcing method can be employed to nullify the undesired symbols. Using the zero-forcing method, the vector  $\mathbf{x}_{eNB}$  can be generated at the eNB by precoding  $\mathbf{d}$  with an  $M \times K$  weight matrix as shown in Equation (6).

$$\mathbf{x}_{eNB} = \mathbf{W}\mathbf{d} \quad (6)$$

where

$$\mathbf{W} = \begin{bmatrix} \omega_{11} & \omega_{12} & \dots & \omega_{1K} \\ \omega_{21} & \omega_{22} & \dots & \omega_{2K} \\ \vdots & \vdots & \ddots & \vdots \\ \omega_{M1} & \omega_{M2} & \dots & \omega_{MK} \end{bmatrix} \quad (7)$$

The weight  $\omega_{mk}$  represents the precoding coefficient allocated by the  $m$ th eNB for the  $k$ th UE. The precoding matrix  $\mathbf{W}$  can be simply obtained by inverting the channel matrix  $\mathbf{H}$ . The capacity of the network MIMO system of  $K$  UEs is the sum of the capacity of each UE which can be obtained from Equation (5). Thus, the sum-rate capacity can be expressed as

$$C_{DN} = \sum_{k=1}^K \log_2 \left( 1 + \frac{|(\mathbf{h}_{DL,k} + gh_{AL,1k} \mathbf{h}_{RL}) \mathbf{w}_k|^2}{|g|^2 |h_{AL,1k}|^2 \sigma_{RN,1}^2 + \sigma_{UE,k}^2} \right) \text{ b/s/Hz} \quad (8)$$

where  $\mathbf{w}_k$  denotes the  $k$ th column of  $\mathbf{W}$  for the  $k$ th UE. The zero-forcing method ensures that interference due to multiuser is cancelled, i.e.,

$$(\mathbf{h}_{DL,k} + gh_{AL,1k} \mathbf{h}_{RL}) \mathbf{w}_i = 0, \quad \forall k \neq i \quad (9)$$

### 3.1.1.2 Uplink capacity

The signal received by the RN is given by

$$\begin{aligned} y_{RN,l} &= \sum_{k=1}^K h_{AL,kl} x_{eNB,k} + n_{RN,l} \\ &= \mathbf{h}_{AL} \mathbf{x}_{eNB} + n_{RN,l} \end{aligned} \quad (10)$$

where  $\mathbf{h}_{AL} = [h_{AL,1l} \ h_{AL,2l} \ \dots \ h_{AL,Kl}]$  is the  $1 \times K$  AL channel vector (where  $h_{AL,kl}$  corresponds to the complex-valued, channel gain between the  $k$ th UE and the RN, which takes into account path loss, shadowing and Rayleigh fading),  $\mathbf{x}_{UE} = [x_{UE,1} \ x_{UE,2} \ \dots \ x_{UE,K}]^T$  is the  $K \times 1$  vector of the transmitted signal ( $x_{UE,k}$  is the signal transmitted by the  $k$ th UE), and  $n_{RN,l}$  is the additive white Gaussian noise observed at RN which is identical to that in Equation (1). The signal received at the  $m$ th eNB is a superposition of all the signals transmitted by all UEs and the RN, which is given by

$$y_{eNB,m} = \sum_{k=1}^K h_{DL,km} x_{UE,k} + h_{RL,lm} g y_{RN,l} + n_{eNB,m} \quad (11)$$

$$= \sum_{k=1}^K (h_{DL,km} + g h_{RL,lm} h_{AL,kl}) x_{UE,k} + (g h_{RL,lm} n_{RN,l} + n_{eNB,m}), \quad m = 1, 2, \dots, M$$

where  $h_{DL,km}$  corresponds to the complex-valued, channel gain (which includes path loss, shadowing and Rayleigh fading) between the  $k$ th UE and the  $m$ th eNB,  $n_{eNB,m}$  is the additive white Gaussian noise with power equals to  $\varepsilon\{|n_{eNB,m}|^2\} = \sigma_{eNB,m}^2$ , and  $g$  is the amplification gain of RN, which is given by

$$g = \sqrt{\frac{P_{RN,l}}{\sum_{k=1}^K P_{UE,k} |h_{AL,kl}|^2 + \sigma_{RN}^2}} > 1 \quad (12)$$

$P_{RN,l} = \varepsilon\{|g y_{RN,l}|^2\}$  and  $P_{UE,k} = \varepsilon\{|y_{UE,k}|^2\}$  are the transmit power of the RN and the  $k$ th UE. Equation (11) can be expressed as

$$y_{eNB,m} = (\mathbf{h}_{DL,m} + g h_{RL,lm} \mathbf{h}_{AL}) \mathbf{x}_{UE} + \tilde{n} \quad (13)$$

where  $\mathbf{x}_{UE}$  is similar to the transmitted signal vector of Equation (10),  $\mathbf{h}_{AL}$  is the AL channel vector as in Equation (10),  $\mathbf{h}_{DL,m} = [h_{DL,1m} \ h_{DL,2m} \ \dots \ h_{DL,Km}]$  is the  $1 \times K$  DL channel vector, and  $\tilde{n} = g h_{RL,lm} n_{RN,l} + n_{eNB,m}$  is effective noise term. The power of the effective noise term is  $\varepsilon\{|\tilde{n}|^2\} = |g|^2 |h_{RL,lm}|^2 \sigma_{RN,l}^2 + \sigma_{eNB,m}^2$ . Finally, we assume that the  $m$ th eNB normalizes  $y_{eNB,m}$  by a factor  $\zeta_m = \sqrt{|g|^2 |h_{RL,lm}|^2 \sigma_{RN,l}^2 + \sigma_{eNB,m}^2}$ . This normalization does not alter the signal-to-noise ratio but simplifies the ensuing presentation.

For  $K$  UEs, we can represent the network MIMO channels in the uplink by a system of linear equations as

$$\underbrace{\begin{bmatrix} y_{eNB,1}/\zeta_1 \\ y_{eNB,2}/\zeta_2 \\ \vdots \\ y_{eNB,M}/\zeta_M \end{bmatrix}}_{\mathbf{y}_{eNB}} = \underbrace{\begin{bmatrix} \frac{1}{\zeta_1} (\mathbf{h}_{DL,1} + g h_{RL,1l} \mathbf{h}_{AL}) \\ \frac{1}{\zeta_2} (\mathbf{h}_{DL,2} + g h_{RL,2l} \mathbf{h}_{AL}) \\ \vdots \\ \frac{1}{\zeta_M} (\mathbf{h}_{DL,M} + g h_{RL,Ml} \mathbf{h}_{AL}) \end{bmatrix}}_{\mathbf{H}} \underbrace{\begin{bmatrix} x_{UE,1} \\ x_{UE,2} \\ \vdots \\ x_{UE,K} \end{bmatrix}}_{\mathbf{x}_{UE}} + \underbrace{\begin{bmatrix} \frac{1}{\zeta_1} (g h_{RL,1l} n_{RN,l} + n_{eNB,1}) \\ \frac{1}{\zeta_2} (g h_{RL,2l} n_{RN,l} + n_{eNB,2}) \\ \vdots \\ \frac{1}{\zeta_M} (g h_{RL,Ml} n_{RN,l} + n_{eNB,M}) \end{bmatrix}}_{\mathbf{n}} \quad (14)$$

The sum-rate capacity is

$$C_{UP} = \log_2 \det \left( \mathbf{I} + \sum_{k=1}^K \mathbf{g}_k \mathbf{g}_k^* P_{UE,k} \right) \text{ b/s/Hz} \quad (15)$$

where  $\mathbf{g}_k$  is the  $k$ th column of  $\mathbf{H}$ , and  $P_{UE,k}$  is the transmit power of the  $k$ th UE which is equal to  $P_{UE,k} = \varepsilon\{|x_{UE,k}|^2\}$ .

### 3.1.2 Capacity of CoMP

The capacity equations for CoMP can be derived in the same manner as in subsection 3.1.1. Unlike the joint technique, CoMP only involves direct transmissions between the UE and the eNB. In the downlink, the signals received by each of the  $K$  UEs can be summarized as

$$\underbrace{\begin{bmatrix} y_{UE,1} \\ y_{UE,1} \\ \vdots \\ y_{UE,K} \end{bmatrix}}_{\mathbf{y}_{UE}} = \underbrace{\begin{bmatrix} \mathbf{h}_{DL,1} \\ \mathbf{h}_{DL,2} \\ \vdots \\ \mathbf{h}_{DL,K} \end{bmatrix}}_{\mathbf{H}} \underbrace{\begin{bmatrix} x_{eNB,1} \\ x_{eNB,2} \\ \vdots \\ x_{eNB,K} \end{bmatrix}}_{\mathbf{x}_{eNB}} + \underbrace{\begin{bmatrix} n_{UE,1} \\ n_{UE,2} \\ \vdots \\ n_{UE,K} \end{bmatrix}}_{\mathbf{n}} \quad (16)$$

where  $\mathbf{x}_{eNB}$  is given by Equation (6),  $\mathbf{h}_{DL,k} = [h_{DL,1k} \ h_{DL,2k} \ \dots \ h_{DL,Mk}]$  is the  $1 \times M$  DL channel vector ( $h_{DL,mk}$  corresponds to the complex-valued, channel gain which includes path loss, shadowing and Rayleigh fading) between the  $m$ th eNB and the  $k$ th UE, and  $n_{UE,k}$  is the additive white Gaussian noise with power equals to  $\varepsilon\{|n_{UE,k}|^2\} = \sigma_{UE,k}^2$ . The sum-rate capacity is obtained from Equation (16) as

$$C_{DN} = \sum_{k=1}^K \log_2 \left( 1 + \frac{|\mathbf{h}_{DL,k} \mathbf{w}_k|^2}{\sigma_{UE,k}^2} \right) \text{ b/s/Hz} \quad (17)$$

In the uplink, the signals received by each of the eNB can be summarized as

$$\underbrace{\begin{bmatrix} y_{eNB,1}/\zeta_1 \\ y_{eNB,2}/\zeta_2 \\ \vdots \\ y_{eNB,M}/\zeta_M \end{bmatrix}}_{\mathbf{y}_{eNB}} = \underbrace{\begin{bmatrix} \frac{1}{\zeta_1} \mathbf{h}_{DL,1} \\ \frac{1}{\zeta_2} \mathbf{h}_{DL,2} \\ \vdots \\ \frac{1}{\zeta_M} \mathbf{h}_{DL,M} \end{bmatrix}}_{\mathbf{H}} \underbrace{\begin{bmatrix} x_{UE,1} \\ x_{UE,2} \\ \vdots \\ x_{UE,K} \end{bmatrix}}_{\mathbf{x}_{UE}} + \underbrace{\begin{bmatrix} \frac{1}{\zeta_1} n_{eNB,1} \\ \frac{1}{\zeta_2} n_{eNB,2} \\ \vdots \\ \frac{1}{\zeta_M} n_{eNB,M} \end{bmatrix}}_{\mathbf{n}} \quad (18)$$

where  $x_{UE,k}$  is the signal transmitted by the  $k$ th UE,  $\mathbf{h}_{DL,m} = [h_{DL,1m} \ h_{DL,2m} \ \dots \ h_{DL,Km}]$  is the  $1 \times K$  DL channel vector with each element  $h_{DL,km}$  corresponds to the complex-valued, channel gain (which includes path loss, shadowing and Rayleigh fading) between the  $k$ th UE and the  $m$ th eNB, and  $n_{eNB,m}$  is the additive white Gaussian noise with power equals to  $\varepsilon\{|n_{eNB,m}|^2\} = \sigma_{eNB,m}^2$ . Similar to Equation (14), the  $m$ th eNB normalizes  $y_{eNB,m}$  by a factor

$\zeta_m = \sigma_{eNB,m}$ . The sum-rate capacity is obtained from Equation (18) and it is identical to Equation (15) with the channel matrix  $\mathbf{H}$  given in Equation (18).

#### 4. Numerical results

In this section, the performance of the proposed joint scheme is evaluated by using Monte Carlo simulations. The parameters of the simulation are given in Table 1. The simulated cluster is composed of two cells. Only one UE was located in each cell. For the AL and DL links, we used the WINNER II C2 - Typical Urban Macro-cell Environment with Non Line-of-Sight (NLOS) channel model (Kyosti et al., 2007). The WINNER II B5a - LOS Stationary

Maximum total transmit power of eNBs	17 dBW
Maximum transmit power of the RN	14 dBW
Maximum total transmit power of UEs	5 dBW
RL (eNB-RN)channel model	WINNER B5a (Kyosti et al., 2007)
DL (eNB-UE) channel model	WINNER C2 NLOS (Kyosti et al., 2007)
AL (RN-UE) channel model	WINNER C2 NLOS (Kyosti et al., 2007)
Number of simulation runs	1000
Cell radius	876 m
Noise power ( $\sigma_{UE,k}^2$ , $\sigma_{RN,l}^2$ and $\sigma_{eNB,m}^2$ )	-144 dBW
Number of eNBs ( $M$ )	2
Number of RN ( $L$ )	1
Number of UE ( $K$ )	2
Height of the eNB	25 m
Height of the RN	25 m
Height of the UE	1.5 m
Carrier frequency	2 GHz
Distance between eNB and UE in the same cell	700 m
Distance between eNB and UE in the different cell	1052 m
Distance between RN and UE	176 m

Table 1. Simulation Parameters

Feeder model (Kyosti et al., 2007) was used for the RL link. For the latter, a strong LOS signal is assumed. The assumption is valid because the position of the RN is fixed and it can be placed in such a way that a strong LOS signal is achieved. The RL channel is almost like in free space. Thus, the path loss does not depend on the antenna heights.

The height of the eNB is similar to the RN is similar, which was set to 25 m in the simulation. The height of the UEs was set to 1.5 m above the ground. The multi-path fading is a Rayleigh distribution. The carrier frequency was set to 2 GHz. The total maximum transmit power of eNB was set to 17 dBW. For simplicity, we assume the power is equally distributed between the two eNBs. The total maximum UE transmit power was set to 5 dBW. Similar to eNB, the power is equally distributed between the two UEs. The noise power ( $\sigma_{UE,k}^2$ ,  $\sigma_{RN,l}^2$  and  $\sigma_{eNB,m}^2$ ) was set to -144 dBW. This noise power level corresponds to a 10-MHz channel.

Fig. 4 shows the downlink sum-rate capacity for the joint scheme and CoMP. The sum-rate capacity is the rate of the two UEs in the cells averaged over 1000 iterations. The joint scheme outperforms the CoMP by more than 4 b/s/Hz. The sum-rates of both schemes increase with higher eNB transmit power because of the higher Signal-to-Noise Ratio (SNR). Uplink sum-rates are given in Fig. 5. As in the downlink case, the performance of the joint scheme is superior to CoMP. The achievable performance gain of the joint scheme is more than 7 b/s/Hz. The performance in the uplink is higher than in the downlink. This is because of the short-range connection between the UE and the RN. The signal received by the RN has very high SNR, which is then amplified and relayed to the eNB through a high quality channel.

Fig. 6 shows the downlink sum-rate for the joint scheme and the CoMP as a function of the UE distance from the RN. Both eNBs were set to transmit at the maximum power. Clearly, joint scheme outperforms CoMP. An interesting observation is made when both UEs are distanced from the RN, the joint scheme delivers a significant performance gain as compared with CoMP. The effect of the RN on the SNR at the receiver is clearly evidenced. The joint scheme benefits from the RN amplification gain and the low noise level of the RL link. Fig. 7 shows the uplink sum-rate for the same techniques. Unlike in the downlink case, the performance of the joint scheme in the uplink degrades as both UEs are distanced from the RN which leads to low SNR of the AL link. The performance degradation of the joint scheme is attributed to the amplified noise received at the RN through the AL link. This noise amplification offsets any gain resulting from using the RN. Thus, CoMP yields superior performance. However, the performance of the joint scheme is still better when the UEs are near the RN.

Figs. 8 and 9 show the downlink and uplink sum-rate capacity as a function of relay transmit power, respectively. The sum-rates of the joint scheme are higher than CoMP. The plots of CoMP are constant because no relays are included in its model. Increasing the transmission power of the RN, the sum-rate is increased by an approximately 0.5 b/s/Hz. The joint scheme gives a roughly 60% and 200% capacity increase relative to CoMP in the downlink and uplink, respectively. The capacity gain in the uplink is higher than in the downlink because of the short-range connection between the UE and the RN which leads to high SNR. Thus, the noise amplification by the RN is minimal as compared with the downlink transmission which has longer range. The joint scheme benefits from both spatial diversity gain and amplification, which are provided by the RN.

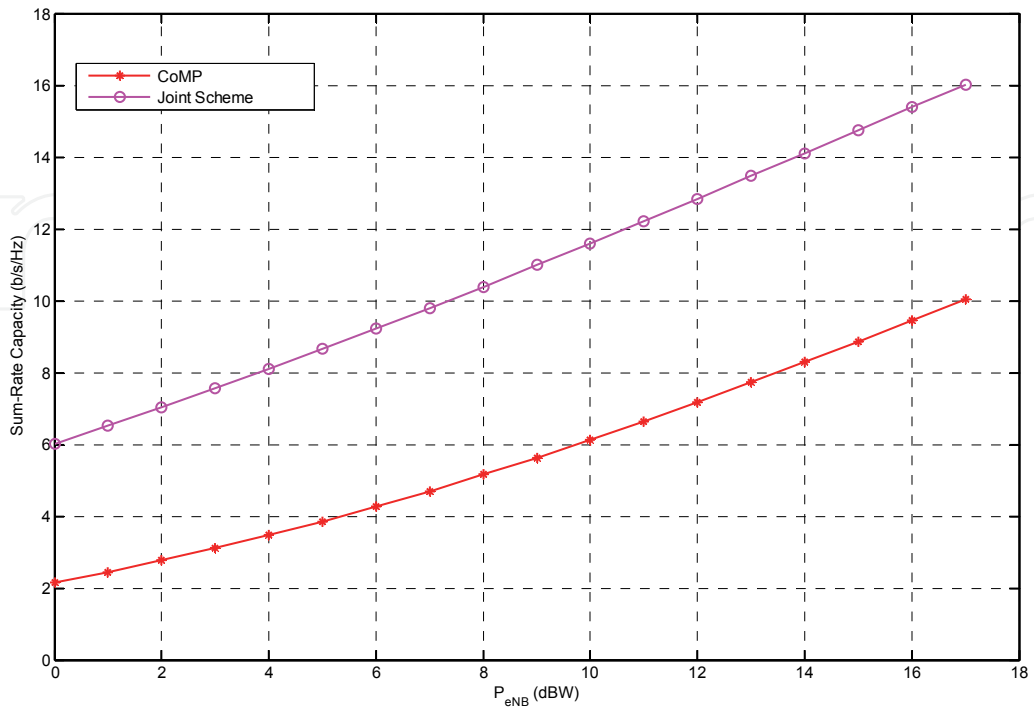


Fig. 4. Sum-Rate Capacity versus  $P_{eNB}$  in the downlink transmission

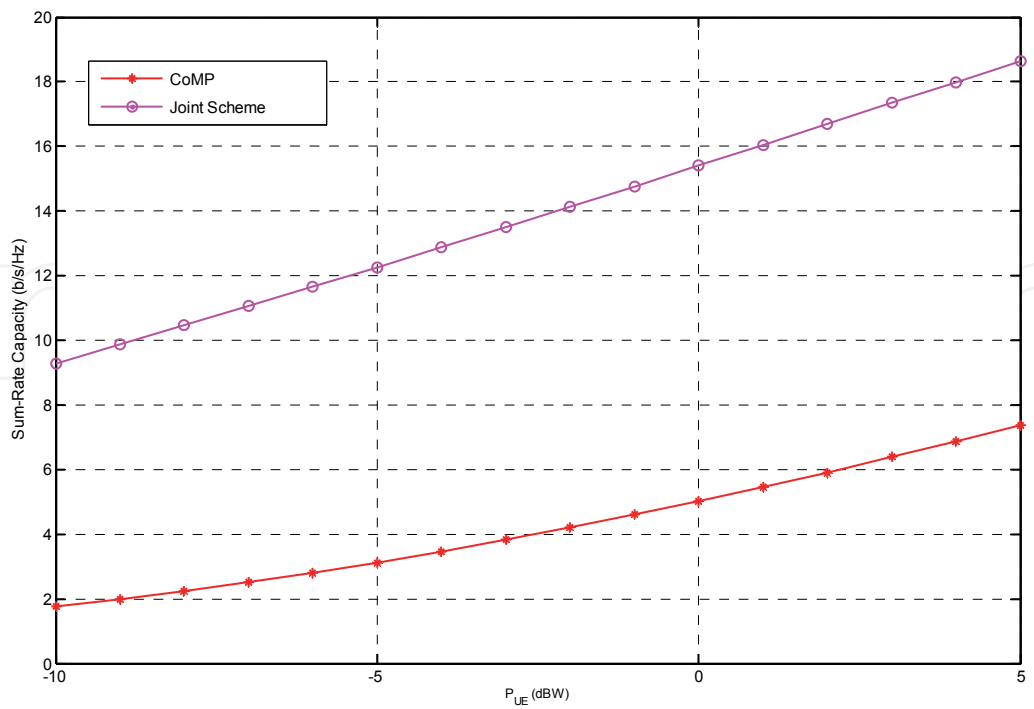


Fig. 5. Sum-Rate Capacity versus  $P_{UE}$  in the uplink transmission

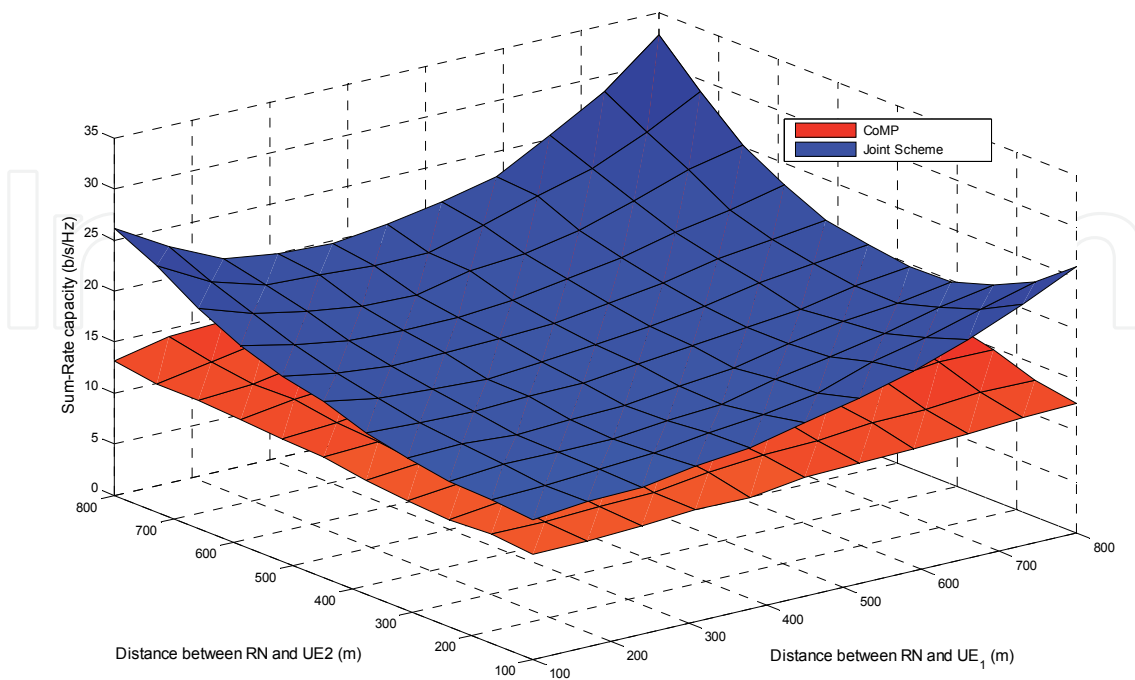


Fig. 6. Sum-Rate Capacity versus the UE distance relative to the RN in the downlink

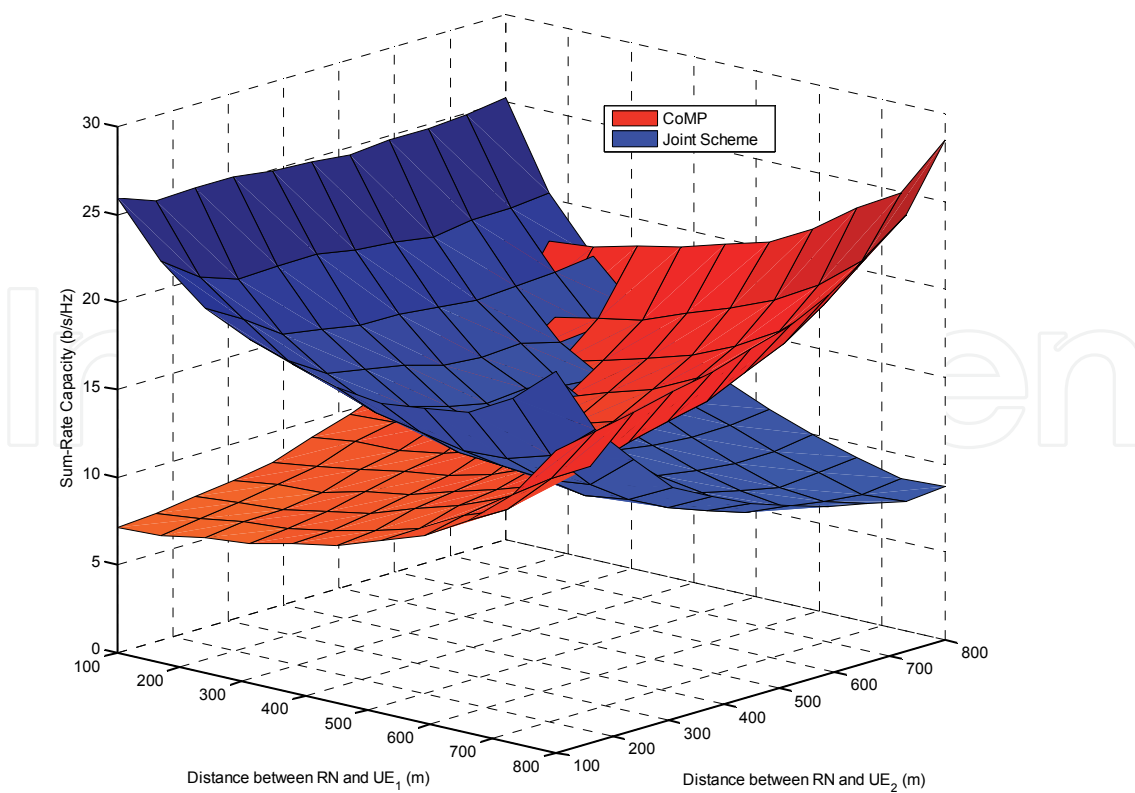


Fig. 7. Sum-Rate Capacity versus the UE distance relative to the RN in the uplink

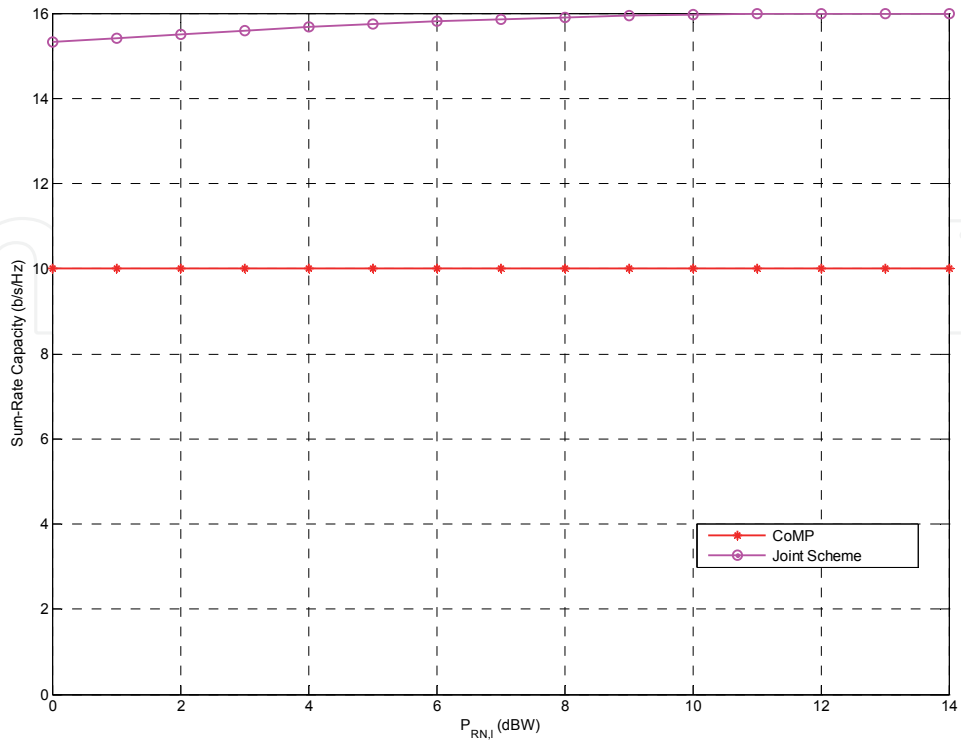


Fig. 8. Sum-Rate Capacity versus  $P_{RN,I}$  in the downlink transmission

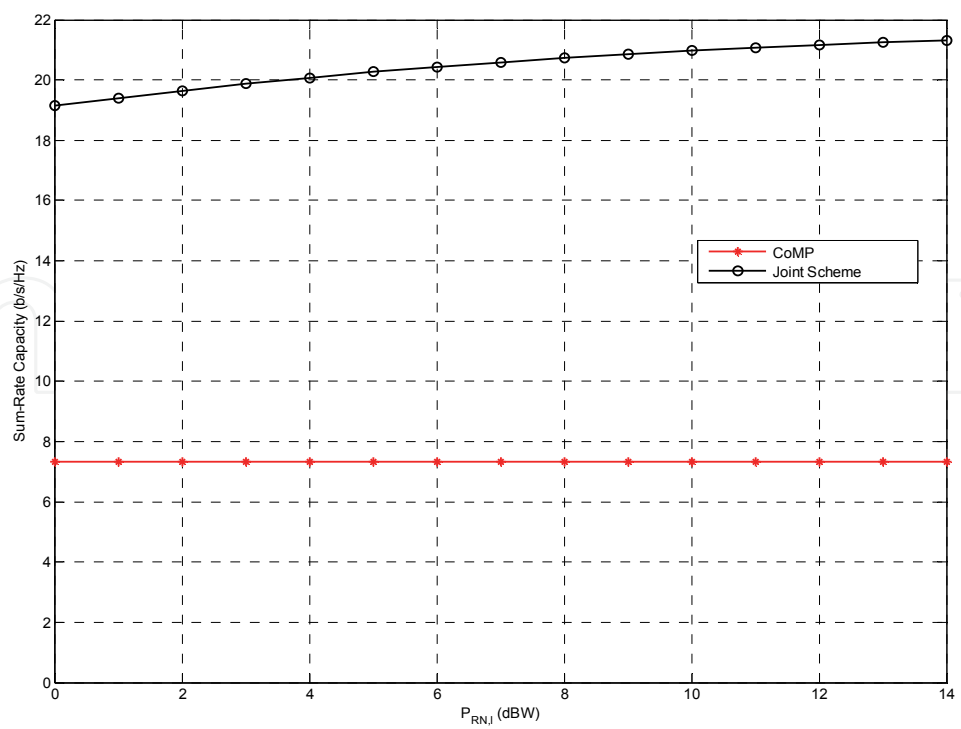


Fig. 9. Sum-Rate Capacity versus  $P_{RN,I}$  in the uplink transmission

## 5. Conclusion

This chapter has proposed a joint cooperative shared relaying and CoMP technique to improve the performance of cell-edge users in LTE-Advanced multi-hop cellular networks. The performance of cell-edge users is severely degraded as a consequence of co-channel interference due to full-frequency reuse. The proposed joint technique considers a full-duplex amplify-and-forward relay due to its high spectral efficiency and low latency. The joint technique supports multi-user transmissions in order to increase system throughput. In the downlink, the relay node amplifies, combines and retransmits the received signals from the intersecting eNodeBs to multiple users. The zero-forcing method was used to nullify the interuser interference at the destination. In the uplink, the relay node amplifies combines and retransmits the received signals from multiple users to all intersecting eNodeBs. In both downlink and uplink, the destination combines the relayed signal and the direct signal from all the sources in order to attain cooperative diversity. We have derived the capacity equations for the joint technique and the CoMP as a baseline for comparison. Numerical results show that the performance of the joint technique is superior to CoMP in both uplink and downlink by at least a factor of three. The results also indicate that the channel quality of the relay link has a strong impact on the downlink performance than in the uplink. Therefore, it is crucial to deploy the relay node in a location that gives the best relay link quality.

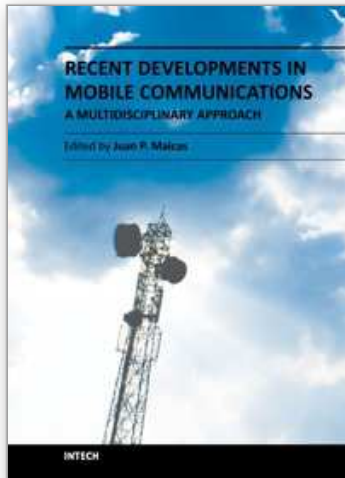
## 6. References

- Berger, S.; Kuhn, M.; Wittneben, A.; Unger, T. & Klein, A. (2009). Recent Advances in Amplify-and-Forward Two-Hop Relaying. *IEEE Communications Magazine*, Vol.47, No.7, (2009)
- Cover, T.M. & El Gamal, A.A. (1979). Capacity Theorems for the Relay Channel. *IEEE Transactions on Information Theory*. Vol.25, No.5, (1979)
- Hoymann, C.; Racz, A.; Johansson, N.; & Lundsjo, J. (2008). A Self-backhauling Solution for LTE-Advanced. *WWRF*, 2008
- Kyosti, P.; et al. (2007). WINNER II Channel Models. IST-4-027756 WINNER II Project, D1.1.2, 2007
- Kramer, G.; Gastpar, M. & Gupta, P. (2005). Cooperative Strategies and Capacity Theorems for Relay Networks. *IEEE Transactions on Information Theory*. Vol.51, No.9, (2005)
- Laneman, J.N.; Tse, D.N.C.; & Wornell, G.W. (2004). Cooperative Diversity in Wireless Networks: Efficient Protocols and Outage Behavior. *IEEE Transactions on Information Theory*, Vol.50, No.12, (2004)
- Loa, K.; Wu, C.; Sheu, S.; Yuan, Y.; Chion, M.; Huo, D. & Xu, L. (2010). IMT-Advanced Relay Standards. *IEEE Communications Magazine*, Vol. 48, No.8, (August 2010)
- Parkvall, S.; Furuskar, A. & Dahlman, E. (2011). Evolution of LTE toward IMT-Advanced. *IEEE Communications Magazine*, Vol.49, No.2 (February 2011)

- Sawahashi, M.; Kishiyama, Y.; Morimoto, A.; Nishikawa, D. & Motohiro, T. (2010). Coordinated Multipoint Transmission/Reception Techniques for LTE-Advanced. *IEEE Wireless Communications*, Vol.17, No.3, (2010)
- 3GPP TR36.814 (2010). Further Advancements for E-UTRA Physical Layer Aspects (Rel 9). 3GPP TR 36.814 V9.0.0, 2010

IntechOpen

IntechOpen



**Recent Developments in Mobile Communications - A  
Multidisciplinary Approach**

Edited by Dr Juan P. Maicas

ISBN 978-953-307-910-3

Hard cover, 272 pages

**Publisher** InTech

**Published online** 16, December, 2011

**Published in print edition** December, 2011

Recent Developments in Mobile Communications - A Multidisciplinary Approach offers a multidisciplinary perspective on the mobile telecommunications industry. The aim of the chapters is to offer both comprehensive and up-to-date surveys of recent developments and the state-of-the-art of various economical and technical aspects of mobile telecommunications markets. The economy-oriented section offers a variety of chapters dealing with different topics within the field. An overview is given on the effects of privatization on mobile service providers' performance; application of the LAM model to market segmentation; the details of WAC; the current state of the telecommunication market; a potential framework for the analysis of the composition of both ecosystems and value networks using tussles and control points; the return of quality investments applied to the mobile telecommunications industry; the current state in the networks effects literature. The other section of the book approaches the field from the technical side. Some of the topics dealt with are antenna parameters for mobile communication systems; emerging wireless technologies that can be employed in RVC communication; ad hoc networks in mobile communications; DoA-based Switching (DoAS); Coordinated MultiPoint transmission and reception (CoMP); conventional and unconventional CACs; and water quality dynamic monitoring systems based on web-server-embedded technology.

**How to reference**

In order to correctly reference this scholarly work, feel free to copy and paste the following:

Anthony Lo and Peng Guan (2011). Joint Cooperative Shared Relaying and Multipoint Coordination for Network MIMO in 3GPP LTE-Advanced Multihop Cellular Networks, Recent Developments in Mobile Communications - A Multidisciplinary Approach, Dr Juan P. Maicas (Ed.), ISBN: 978-953-307-910-3, InTech, Available from: <http://www.intechopen.com/books/recent-developments-in-mobile-communications-a-multidisciplinary-approach/joint-cooperative-shared-relaying-and-multipoint-coordination-for-network-mimo-in-3gpp-lte-advanced>

**INTECH**  
open science | open minds

**InTech Europe**

University Campus STeP Ri  
Slavka Krautzeka 83/A  
51000 Rijeka, Croatia  
Phone: +385 (51) 770 447

**InTech China**

Unit 405, Office Block, Hotel Equatorial Shanghai  
No.65, Yan An Road (West), Shanghai, 200040, China  
中国上海市延安西路65号上海国际贵都大饭店办公楼405单元  
Phone: +86-21-62489820

Fax: +385 (51) 686 166  
www.intechopen.com

Fax: +86-21-62489821

IntechOpen

IntechOpen

© 2011 The Author(s). Licensee IntechOpen. This is an open access article distributed under the terms of the [Creative Commons Attribution 3.0 License](#), which permits unrestricted use, distribution, and reproduction in any medium, provided the original work is properly cited.

IntechOpen

IntechOpen